Blood pulse wave velocity measured by photoacoustic microscopy

Chenghung Yeh, Song Hu, Konstantin Maslov, Lihong V. Wang

Chenghung Yeh, Song Hu, Konstantin Maslov, Lihong V. Wang, "Blood pulse wave velocity measured by photoacoustic microscopy," Proc. SPIE 8581, Photons Plus Ultrasound: Imaging and Sensing 2013, 85812C (4 March 2013); doi: 10.1117/12.2004232

SPIE.

Event: SPIE BiOS, 2013, San Francisco, California, United States

Blood Pulse Wave Velocity Measured by Photoacoustic Microscopy

Chenghung Yeh†, Song Hu†, Konstantin Maslov, and Lihong V. Wang*
Optical Imaging Laboratory, Department of Biomedical Engineering, Washington University in St. Louis, One Brookings Drive, St. Louis, MO 63130, USA
† The authors contributed equally to this work.
* Address all correspondence to: LHWANG@WUSTL.EDU

Abstract

Blood pulse wave velocity (PWV) is an important indicator for vascular stiffness. In this letter, we present electrocardiogram-synchronized photoacoustic microscopy for in vivo noninvasive quantification of the PWV in the peripheral vessels of mice. Interestingly, strong correlation between blood flow speed and ECG were clearly observed in arteries but not in veins. PWV is measured by the pulse travel time and the distance between two spot of a chose vessel, where simultaneously recorded electrocardiograms served as references. Statistical analysis shows a linear correlation between the PWV and the vessel diameter, which agrees with known physiology.
Keywords: photoacoustic microscopy, photoacoustic spectroscopy, bilirubin, scattering medium.

1. Introduction

Cardiovascular diseases, such as hypertension and atherosclerosis, change arterial compliance [1,2] and resistance, altering pulse wave velocity (PWV) [3]. Among indicators of arterial diseases, PWV has been used in evaluating vascular disease as a gold standard because of its reliability and lots of evidence relating it with cardiovascular diseases [2]. Thus, accurate *in vivo* measurement of PWV is of physiological and clinical significance.

Traditional imaging modalities, such as ultrasound imaging and laser Doppler velocimetry, have been adopted for vascular imaging as well as PWV. However, the drawbacks of these techniques include low sensitivity, poor spatial resolution, and the need for surgical preparation to achieve a sufficient signal-to-noise ratio (SNR). Photoacoustic microscopy (PAM), which combines optical imaging with ultrasound in a single modality, has been used for noninvasive, *in vivo* biomedical studies. PAM, which enables high, label-free contrast with optical resolution, can overcome these limitations. Recently, PAM has been reported to measure blood flow and used to measure flow velocity at a single point [4]. However, PWV requires the measurement of multiple points. In this paper, by combining PAM with electrocardiography (ECG), we report performing PWV measurements *in vivo* in the nude mouse ear.

2. System and Materials

Pulse wave velocity (PWV) is determined by

$$PWV = \Delta S / \Delta t ,$$

where Δt is the difference of red blood cell (RBC) velocity at two sites for a given time lag, and ΔS is the distance between the two sites.

The difference in flow velocity at subsequent locations along a single vessel is calculated by maximizing the cross-covariance function, $CV(\tau)$, written as

$$CV(\tau) = E\{[V_1(t) - \mu_1][V_2(t-\tau) - \mu_2]\} ,$$

Photons Plus Ultrasound: Imaging and Sensing 2013, edited by Alexander A. Oraevsky, Lihong V. Wang,
Proc. of SPIE Vol. 8581, 85812C · © 2013 SPIE · CCC code: 1605-7422/13/$18 · doi: 10.1117/12.2004232

where τ is the time lag between the two signals, t is time, E is the expected value, V is an RBC velocity of the ensemble average, and μ is the expected value of V. To accurately quantify PWV, we select measurement segments along vessels without branch points.

The dual-modal system consists of a second-generation optical-resolution PAM (OR-PAM) system [5] and a home-made ECG recorder (Fig. 1). In OR-PAM, the outputs of a solid-state laser (SPOT, Elforlight) and a wavelength-tunable laser system (pump laser: INNOSLAB, Edgewave; dye laser: CBR-D, Sirah) were combined using a beam splitter to provide pulse-to-pulse wavelength switching for the measurement of hemoglobin oxygen saturation (sO_2). The combined laser beam was spatially filtered by an iris (ID25SS, Thorlabs; aperture size: 2 mm), focused by a condenser lens (LA1131, Thorlabs) through a 50-μm-diameter pinhole (P50C, Thorlabs), and then coupled into a single-mode fiber (PA-460A-FC-2, Thorlabs). A tunable neutral density filter (NDC-50C-2M, Thorlabs) was placed before the fiber coupler to regulate the intensity of the incident beam. The fiber output was collimated by a microscope objective (RMS4X, Thorlabs), reflected by a mirror, and re-focused by a second identical objective to achieve nearly diffraction-limited optical focusing (focal diameter: 2.6 μm). A home-made acoustic-optical beam combiner, containing an oil-filled interface, was placed beneath the objective to align the optical excitation and ultrasound detection coaxially and confocally. The generated photoacoustic wave was focused by an acoustic lens, detected by an unfocused ultrasonic transducer (V214-BB-RM, Olympus-NDT), and amplified by two 24-dB cascaded electrical amplifiers (ZFL 500LN, Mini-Circuits). Electrocardiograms were simultaneously recorded with three electrodes connected to the ground and to a front and a hind leg of a mouse, and then amplified by a high-gain differential amplifier (Model 3000, A-M systems). The acquired photoacoustic and ECG signals were digitized by a dual-channel high-resolution digitizer (NI PCI 5124, National Instruments Corporation).
The experimental mouse (Hsd: Athymic Nude-Fox1^{nu}, Harlan Co.) was anesthetized with 1.2% isoflurane vaporized by a breathing anesthesia system (E-Z Anesthesia, Euthanex) for *in vivo* experiments. All experimental animal procedures were carried out in conformity with the laboratory animal protocol approved by the Animal Studies Committee of Washington University in St. Louis.

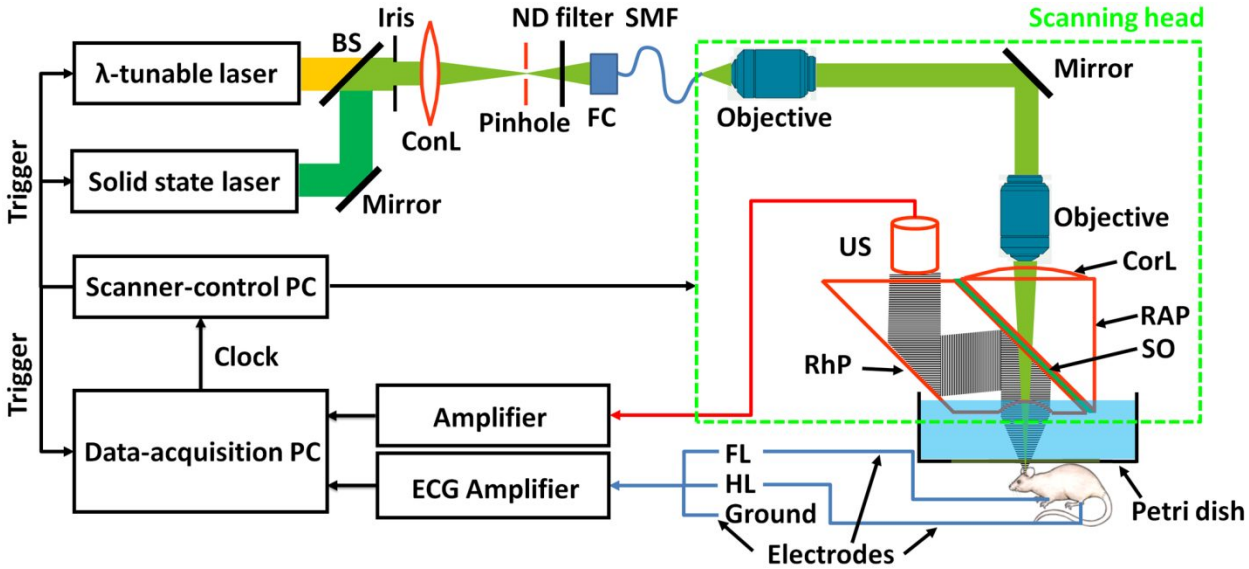

Fig. 1. Schematic of the ECG-synchronized OR-PAM system for PWV measurement. λ, wavelength; BS, beam splitter; ConL, condenser lens; ND, neutral density; FC, fiber collimator; SMF, single-mode fiber; CorL, correction lens; RAP, right-angle prism; SO, silicone oil; RhP, rhomboid prism; US, ultrasonic transducer; FL, foreleg; HL, hind leg; PC, personal computer.

3. Experiments and Results

3.1 Hemoglobin Oxygen Saturation and Flow Velocity

Using the method described in previous work [5], we utilized photoacoustic images at wavelengths of 532 nm and 561 nm. By the molar absorption coefficients of oxyhemoglobin and deoxyhemoglobin, the hemoglobin oxygen saturation (sO2) of the whole-ear vasculature network is quantified. Figure 2 shows the resulting sO2 map, where the arteries are the vessels with high sO2 values (>85%) and veins are the vessels with low sO2 values (85 to 65%) [6]. To quantify the RBC flow velocity in both arteries and veins, we selected a B-scan by using the sO2 map. We used the full width at half maximum (FWHM) value of the blood vessel PA signal from each B-scan to estimate the diameter of the vessel. For the representative artery (A) and vein (V) indicated in Fig 2, simultaneous measurements of RBC flow velocity and ECG (Fig 3a,b) were made. The transverse RBC velocity in the artery and vein was M-mode measured by Doppler broadening of PA bandwidth [4]. The corresponding power spectra of the RBC velocity and the ECG, shown in figures 3c and 3d, were calculated by a fast Fourier transform (FFT) with a sampling rate of 1530.

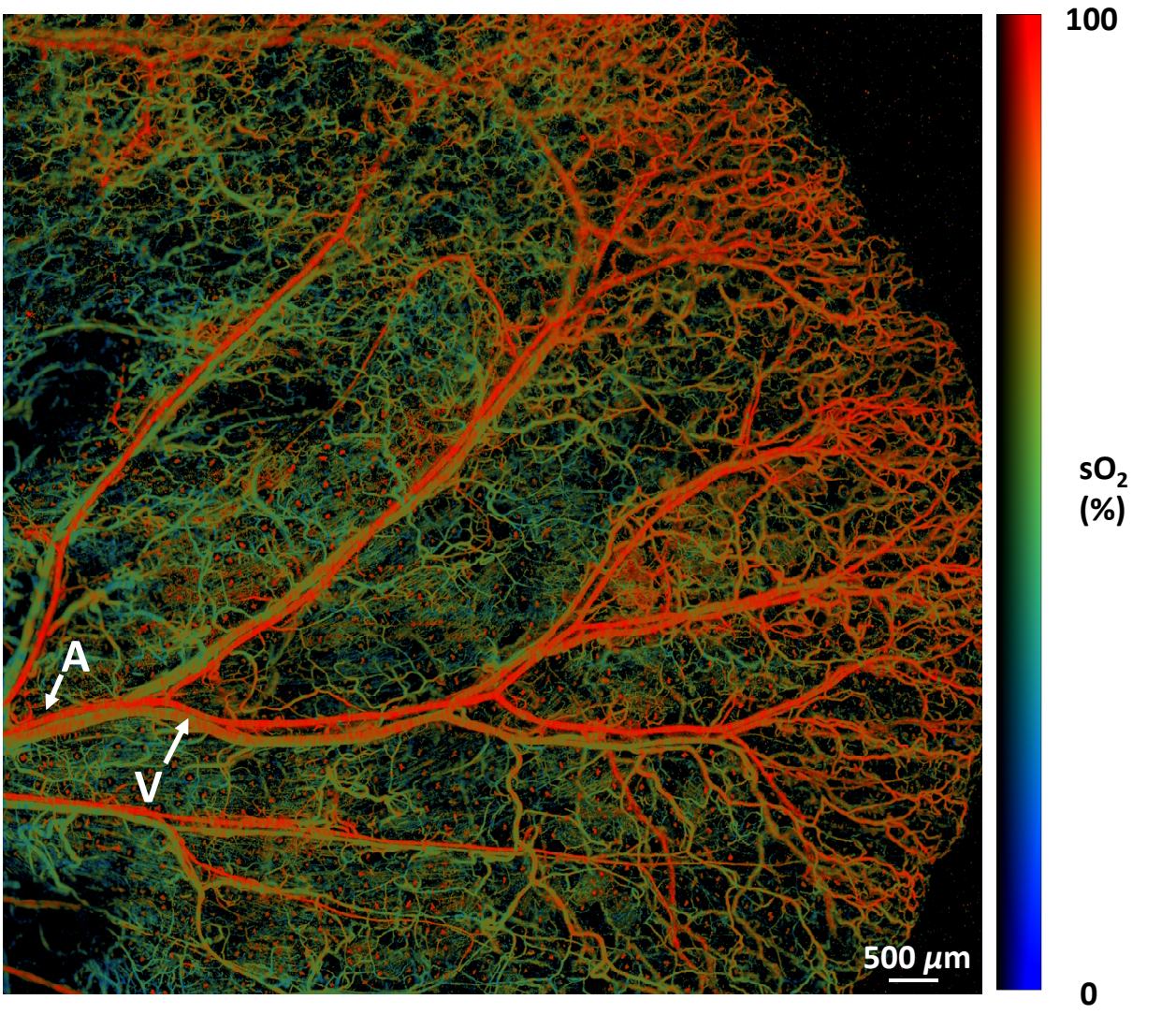

Fig. 2. Differential responses of artery and vein to cardiac pulsation. Dual-wavelength (532 nm and 563 nm) OR-PAM of sO_2 in a nude mouse ear. A, a cross section in the artery; V, a cross section in the vein.

3.2 Pulse Wave Velocity

Four-step 1uantification of pulse wave velocity are applied[7]. We defined the ensemble averaged RBC velocity by using the ECG as a reference signal. A typical ECG signal consists of a P wave, a T wave, a U wave, and a QRS complex. Each peak of a P wave, set as a starting point, plus an average heart beat duration (186 ms), formed a pair

of the ECG signal and its corresponding RBC velocity. In the subsequent intervals, we divided the paired signal into multiple single-period segments and averaged 170 single-period segments as the RBC flow pattern. To improve the accuracy of the ensemble average, we set a criterion by calculating the autocovariance value between the ensemble average flow pattern and each single-period segment. The signals with low autocovariance coefficients (< 0) were discarded, whereas the signals with high autocovariance coefficients (> 0) were saved as a refined the ensemble average flow velocity. By the cross-covariance method mentioned above, pulse wave velocity is calculated from refined ensemble flow velocity signals at the two sequential points.

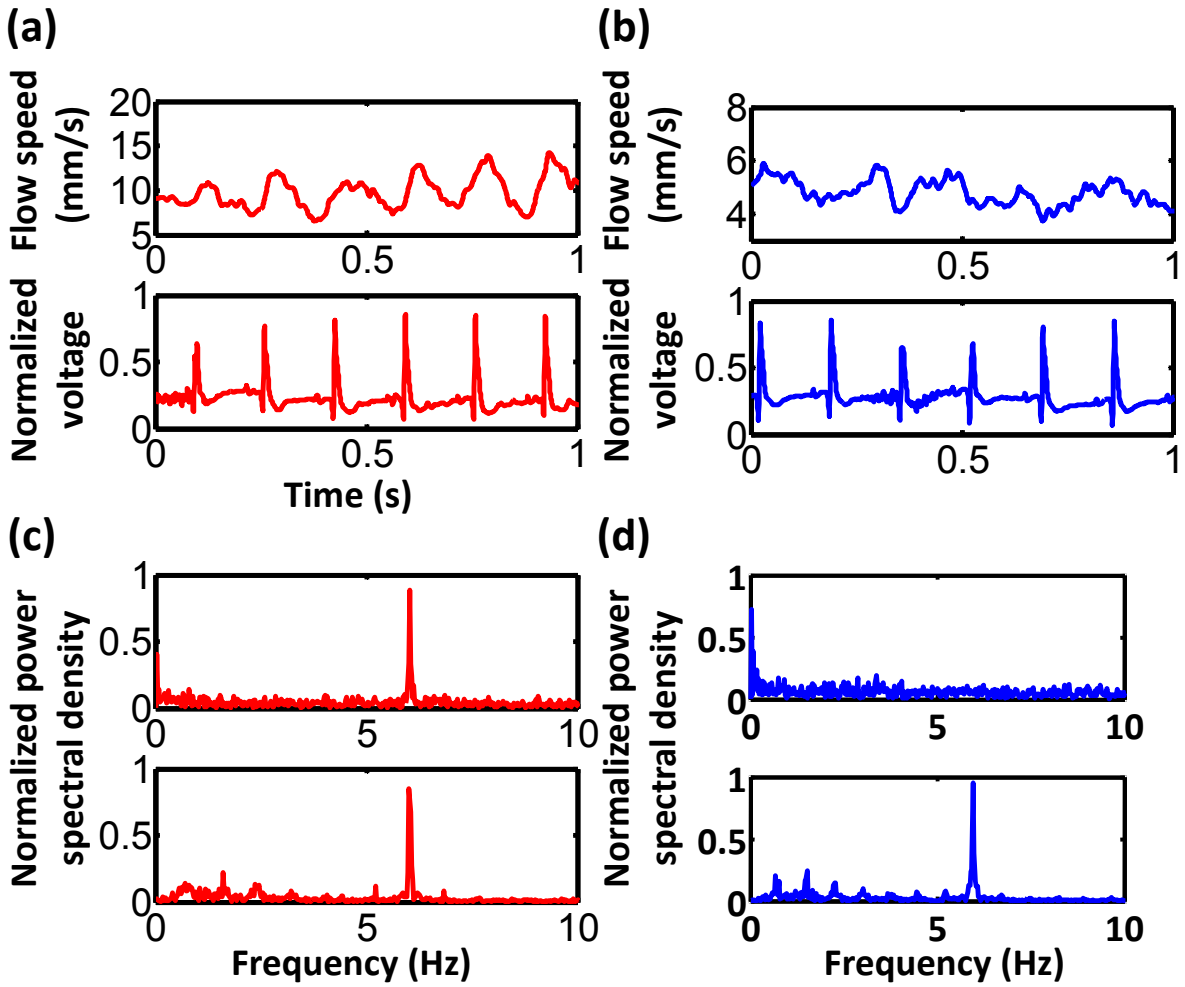

Fig. 3. (a) Simultaneous measurements of the arterial flow speed at cross section A (top) and ECG (bottom). (b) Simultaneous measurements of the venous flow speed at cross section V (top) and ECG (bottom). (c) Normalized power spectra of the arterial flow speed (top) and ECG (bottom) signals shown in (a). (d) Normalized power spectra of the venous flow speed (top) and ECG (bottom) signals shown in (b).

In the artery, the RBC velocity (shown in Fig 2a) exhibited pulsatile fluctuation in the time domain. The power spectrum of RBC velocity (Fig 2c) also showed a peak at pulsatile frequency (~ 6Hz) with a high SNR (15.75). The power spectrum of the rest points in arteries also suggested that the RBC velocity in arteries was strongly correlated with ECG. In contrast, the RBC velocity in the vein had no pulsatile fluctuation in either the time domain or the power spectrum. The corresponding amplitude peak at the frequency of the pulsation showed low SNR (0.40). This observation is consistent with the results reported by Okada et al. [8], and can be explained by the nature of arteries and veins. Blood is pumped out of the heart and enters the arteries, which supply the capillaries. The RBCs gradually lose their momentum through systemic circulation, and are collected by veins, which return blood to the heart with help from the skeletal-muscle pump. Blood in an artery is actively transported by heart motion (heart beat

correlated); whereas blood transport in a vein is passively regulated by valves and driven by the skeletal-muscle pump (both heart beat uncorrelated). In Figures 2c and 2d, note that there are several peaks in the spectrum at lower frequencies (0 to 4 Hz) in both arteries and veins. These peaks suggest that ECG and RBC velocity are affected by respiration, vasomotion and other slow variations.

In light of these findings, we neglected the veins and measured PWV at several sites along arteries. Fig 4 shows PWV plotted against artery vessel diameter. The data set is separated into five groups: 20-30 μm, 30-40 μm, 40-50 μm, 50-60 μm and larger than 60 μm. The outlier at the diameter of 79 μm was discarded for fitting by linear regression. The slope of linear regression was about 2.1, within the range of values reported in the literature [9,10].

Complementary to ultrasonic measurements of PWV in the aorta, OR-PAM is capable of measuring the PWV in peripheral microvessels. According to the Moens-Korteweg equation [2], PWV is closely associated with vascular stiffness, vessel wall thickness, and blood density. This innovation holds the potential to study a broad range of peripheral cardiovascular diseases, including diabetes and hypertension, by providing a metric of local vascular stiffness and blood pressure. Extending this method to intravascular photoacoustic endoscopy can potentially enable early diagnosis of arteriosclerosis [11]. Furthermore, combining PWV with previously quantified vascular anatomy, sO_2, blood flow, and the metabolic rate of oxygen can provide a comprehensive characterization of cardiovascular diseases.

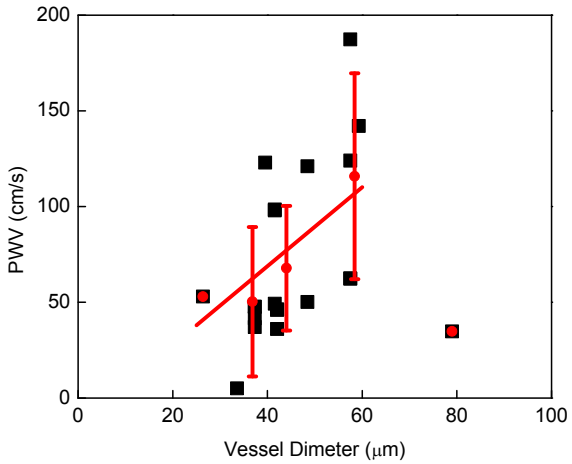

Fig. 4. Pulse wave velocity (■) in arterioles of nude mice ears. Pulse wave velocity averaged over vessel diameters 20-30 μm, 30-40 μm, 40-50 μm, 50-60 μm and larger than 60 μm are represented by the circle symbol (●) with error bars.

4. Conclusion

In conclusion, we have demonstrated, for the first time, an ECG-synchronized photoacoustic method for noninvasive measurements of the PWV in mouse peripheral microvessels. Strong correlations between the simultaneously recorded ECG and the blood flow patterns were observed in arteries and arterioles but not in veins and venules. Furthermore, a linear relationship between PWV and vessel diameter was observed experimentally, which is in good agreement with the data in the literature.

Acknowledgments

The authors appreciate the close reading of the manuscript by Profs. James Ballard, Seema Dahlheimer, and Lynnea Brumbaugh. Thanks to Amy Winkler and Brian Soetikno for helpful discussions. Thanks to Di Lang for experimental assistance. This work was sponsored by National Institutes of Health Grants R01 EB000712, R01 EB008085, R01 CA134539, U54 CA136398, R01 CA157277, and R01 CA159959. L.V.W. has financial interests in

Microphotoacoustics, Inc. and Endra, Inc., which, however, did not support this work. K. Maslov has a financial interest in Microphotoacoustics, Inc.

Reference

1. Reddy, A.K., et al., *Multichannel Pulsed Doppler Signal Processing for Vascular Measurements in Mice.* Ultrasound in Medicine; Biology, 2009. **35**(12): p. 2042-2054.
2. Nichols, W.W., M.F. O'Rourke, and C. Vlachopoulos, *McDonald's Blood Flow in Arteries: Theoretical, Experimental and Clinical Principles*. 2011: Oxford Univ Pr.
3. Lakatta, E.G., et al., *Human aging: Changes in structure and function.* Journal of the American College of Cardiology, 1987. **10**(2, Supplement 1): p. 42A-47A.
4. Yao, J., et al., *In vivo photoacoustic imaging of transverse blood flow by using Doppler broadening of bandwidth.* Optics letters, 2010. **35**(9): p. 1419-1421.
5. Hu, S., K. Maslov, and L.V. Wang, *Second-generation optical-resolution photoacoustic microscopy with improved sensitivity and speed.* Opt. Lett., 2011. **36**(7): p. 1134-1136.
6. Yao, J., et al., *Label-free oxygen-metabolic photoacoustic microscopy in vivo.* Journal of Biomedical Optics, 2011. **16**: p. 076003.
7. Yeh C., et al., Photoacoustic microscopy of blood pulse wave, Journal of Biomedical Optics **17** (7), 070504 (2012).
8. Okada, E., et al. *Spectrum analysis of fluctuations of RBC velocity in microvessels by using microscopic laser Doppler velocimetry*. in *Engineering in Medicine and Biology Society, 1989. Images of the Twenty-First Century., Proceedings of the Annual International Conference of the IEEE Engineering in*. 1989.
9. Okada, E., et al. *Application Of Microscopic Laser Doppler Velocimeter For Analysis Of Arterial Pulse Wave In Microcirculation*. in *Engineering in Medicine and Biology Society, 1990., Proceedings of the Twelfth Annual International Conference of the IEEE*. 1990.
10. Seki, J., *Flow pulsation and network structure in mesenteric microvasculature of rats.* American Journal of Physiology-Heart and Circulatory Physiology, 1994. **266**(2): p. H811.
11. Chubachi, N., et al. *Measurement of local pulse wave velocity in arteriosclerosis by ultrasonic Doppler method*. 1994: IEEE.